White Rose Research Online

eprints@whiterose.ac.uk
https://eprints.whiterose.ac.uk
Universities of Leeds, Sheffield and York

Deposited via The University of Sheffield.

White Rose Research Online URL for this paper:
https://eprints.whiterose.ac.uk/id/eprint/199109/

Version: Accepted Version

Article:
Gaetano, D.D., Zhu, W., Sun, X. et al. (2023) Experimental ball bearing impedance analysis under different speed and electrical conditions. IEEE Transactions on Dielectrics and Electrical Insulation, 30 (3). pp. 1312-1321. ISSN: 1070-9878

https://doi.org/10.1109/tdei.2023.3271958

© 2023 The Authors. Except as otherwise noted, this author-accepted version of a journal article published in IEEE Transactions on Dielectrics and Electrical Insulation is made available via the University of Sheffield Research Publications and Copyright Policy under the terms of the Creative Commons Attribution 4.0 International License (CC-BY 4.0), which permits unrestricted use, distribution and reproduction in any medium, provided the original work is properly cited. To view a copy of this licence, visit http://creativecommons.org/licenses/by/4.0/

Reuse
This article is distributed under the terms of the Creative Commons Attribution (CC BY) licence. This licence allows you to distribute, remix, tweak, and build upon the work, even commercially, as long as you credit the authors for the original work. More information and the full terms of the licence here: https://creativecommons.org/licenses/

Takedown
If you consider content in White Rose Research Online to be in breach of UK law, please notify us by emailing eprints@whiterose.ac.uk including the URL of the record and the reason for the withdrawal request.

UNIVERSITY OF LEEDS
University of Sheffield
UNIVERSITY of York

Experimental Ball Bearing Impedance Analysis Under Different Speed and Electrical Conditions

Daniele De Gaetano, Wenjun Zhu, Xiangyu Sun, Xiao Chen, Antonio Griffo, and Geraint W Jewell

***Abstract*—Ball bearings are commonly used in inverter driven electrical machines, where they can be subject to high frequency common mode currents which accelerate their degradation. This paper investigates the impact of shaft speed, voltage amplitude and frequency on the bearing impedance, including during electrical discharges, with the aim to provide an experimentally validated approach to model their high frequency behaviour as function of operating conditions. This analysis can help the development of improved models to predict bearing currents in electric drives. A dedicated experimental setup, completely isolated from ground, is presented. It proposes dielectric plate and bolts to insulate the bearing from the support (which is connected to the ground), a dielectric coupling to insulate the dyno from bearing, dielectric sheets to insulate the brush holder from the ground. Different voltage and frequency amplitudes are applied between the inner and outer bearing raceways for several shaft speeds. The measured impedance amplitude and phase, currents and voltages are presented. Due to the large amount of data, a statistical approach is proposed for studying the bearings behaviour. A simple analytical bearing model is presented in order to provide an interpretation of the experimental measurements. The analysis shows that the voltage amplitude and frequency have a significant impact on electrical discharge in ball bearings, especially for certain shaft speeds strongly affecting the impedance amplitude and phase during the breakdown state.**

***Index Terms*—Ball bearings, Current measurement, Dielectric breakdown, Discharges, Electric machines, Impedance, Motor drives, Variable speed drives, Voltage measurement.**

I. Introduction

PREMATURE electrical machine bearing failures are often associated to the circulation of high frequency parasitic bearing currents. The source of these bearings currents is the common-mode voltage V_{COM}, generated by inverter's switches [1]-[2]-[3]. Modern PWM inverters with switching frequencies of tens of kHz and high dv/dt often in excess of $10kV/\mu s$ produce a wide spectrum V_{COM}, with components from kHz to MHz, which, in turns, produce wide spectrum common mode currents, which can partially circulate in the bearings, contributing to their degradation. In particular, V_{COM} affects electrical machines driven by three-phase inverters where there are not enough freedom degrees to balance the applied voltage.

Manuscript created July, 2022; This work is supported by the U.K. EPSRC through research award EP/W015838/1. For the purpose of open access, the authors have applied a Creative Commons Attribution (CC BY) license to any Author Accepted Manuscript version arising.

Daniele De Gaetano, Wenjun Zhu, Xiangyu Sun, Xiao Chen, Antonio Griffo and Geraint W Jewell are within the Department of Electronic and Electrical Engineering, The University of Sheffield, Sheffield, U.K.. Corresponding author: Xiao Chen (e-mail: xiao.chen@sheffield.ac.uk).

Understanding the frequency characteristic of the bearings, as well as the effect of other operating conditions such as shaft speed and voltage amplitude, is essential to correctly predict the bearings currents and identify potential mitigation solutions.

Many techniques to mitigate bearing currents from the inverter ([4]-[9]) and motor sides ([10]-[14]) have been proposed.

Bearing currents can be classified based on the underlying physical mechanisms. The main two are the circulating and electrical discharge machining (EDM) currents. A comprehensive review is proposed in [15].

Many articles have been published on EDM currents and their impact on the bearings. An investigation of the load and temperature influence on EDM currents is proposed in [16], where it is shown that machines under load are less affected by these impulsive currents, increasing the bearing life. The influence on EDM currents of the impedance of ball bearings is presented by Y. Gemeinder et all. in [17]. In [18], authors propose a study of the bearing impedance proprieties for different operating conditions, showing that its behaviour alternates between capacitive and ohmic without any modification of macroscopic conditions for some of these. Calculation of roller and ball bearing capacitances and the prediction of EDM currents is proposed in [19], highlighting how its accuracy is influenced by the onset of the lubricant's breakdown. Capacitances and lubricant film thickness of motor bearing under different operating conditions are investigated also in [20], showing the influence of temperature and speed on these parameters. Usually, the bearing is modelled as a pure resistance in breakdown and as a pure capacitance in non-breakdown conditions. In [21], the breakdown impedance is modelled as a variable resistance, based on the arc discharge model principle.

The measurements of this high frequency parasitic currents and impedance are challenging. A simplified approach is proposed in [22] where external bearing are used to provide a current path. However, they could have different electric characteristics compared with the motor bearings due to the presence of a load. The use of Rogowsky coils on the shaft can be a method to measure the current in the shaft without affecting the path for the current in the machine. However, a hollow shaft is used for the purpose of providing space for cabling, limiting its applicability [23]-[25]. A radio frequency measurement method to detect bearing currents is implemented in [26]. It is a non-invasive method but it requires a strict electromagnetic shielding, hence no easy implementation. Ref. [27] proposed a method for detecting the gradual fault in the outer race of an induction motor hybrid bearings based on the

stray flux signals acquired around the motor case. For early fault identification, a dynamic degradation monitoring method, which used a variational mode decomposition based trigonometric entropy measure, was reported in [28]. A Review of Artificial Intelligence Methods for Condition Monitoring and Fault Diagnosis of Rolling Element Bearings for Induction Motor was proposed in [29]. Ref. [30] proposed testing a ball bearing by itself, in order to quantify the influence of load, temperature and shaft speed. Measuring and characterising the bearing impedance as a function of the operating conditions is important for understanding its behaviour and providing a model that can be used in the prediction of bearings currents. The impedance properties especially during the breakdown state, have not been analysed in details. This paper presents a systematic measurement methodology and a statistical analysis of the bearings impedance and currents as function of shaft speed, applied voltage amplitude and frequency, up to 1MHz, covering a wide spectrum covering the range of V_{COM} for typical PWM converters. A direct experimental test is proposed where the bearings are isolated from any other conductive path, avoiding any external influence on the impedance measurement. Indeed, the bearings are mounted directly in a specifically designed non conductive holder and coupled with the dynamometer shaft by a non conductive coupling. This approach results in an improved accuracy in the impedance bearings measurement. A statistical approach is used to process the large amount of measured data, focusing on the impedance value in breakdown, breakdown probability, effect of the electrical frequency in breakdown and voltage breakdown point. To complement the proposed experimental set-up and measurements and provide a physical interpretation of the data, a bearing model is implemented. Finally, a summary of the main observed physical phenomenon, obtained by experimental tests, is proposed in the conclusion section. Several ball bearing topologies are available for rotating electrical machines such as angular contact, deep groove, single or double row. They can also vary in terms of used lubricant which is usually grease or oil, as well whether a cover is present or not and, if so, it is can present contact seals or not. This article investigates the impedance behaviour under different speed and electrical conditions of bearing SKF 61905 2RS1 which has the following characteristics: deep groove; single row bearing; lubricated by grease; seal cover, which is in contact. Additional characterisation is carried out for the bearing SKF 61905 R-2Z, which presents the same characteristic except that it has non-contact cover. This means that it has a lower friction than its counterpart with the contacting cover. The validation process and main analyses are carried out for the bearing SKF 61905 2RS1 (higher friction) whereas SKF 61905 R-2Z (lower friction) is used as analysis support. The main novelties of this article are the experimental setup and the impedance analysis not only under normal operating conditions but also in the breakdown state. This experimental setup eliminates a large portion of measurement noise, giving rise to more reliable data which is direct linked to an improved understanding of the bearing impedance behaviour, than would be achieved by studying the bearing by itself. Therefore, this work presents several important additions compared to prior

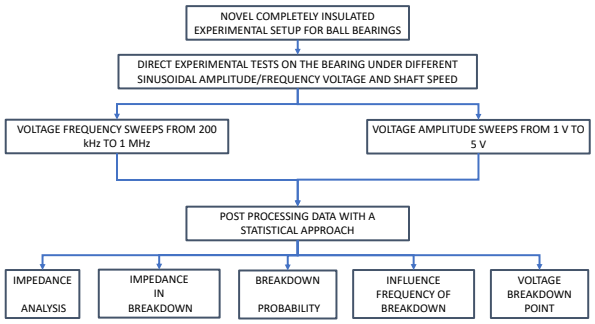

Fig. 1: Block diagram about analysis approach and outputs.

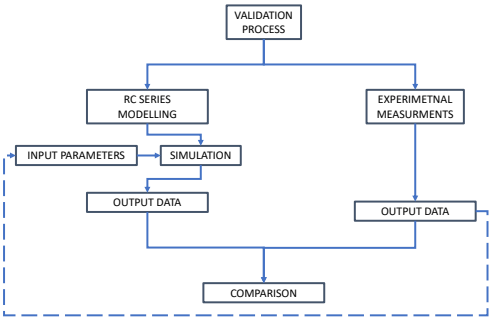

Fig. 2: Block diagram about validation process.

literature:

- Study the bearing by itself, taking into the account many precautions by insulations to reduce the measurements noises;
- Statistical approach adopted on a significant quantity of data to generalise different trends;
- RC series modeling for the validation process;
- Impedance behaviour analysis also during the breakdown state;

Block diagrams illustrating analysis approach, outputs and validation process used in this papers are shown in Fig. 1 and 2, respectively. Fig. 1 shows in detail the two different impedance analyzer settings to detect the bearing impedance values and the post-processing analyses using a statistical approach, while Fig. 2 displays in detail the proposed validation process which uses the experimental test output data as input parameters for the simulation model; the comparison between simulation and experimental test is carried out using the current and voltage output data in both breakdown and no-breakdown conditions.

II. Bearing Impedance Background

Ball bearings are constructed with a number of balls running in between the bearings inner and outer raceways. During rotation of the bearing, there is a thin lubrication oil film between balls and raceways. This oil exhibits dielectric behaviour which results in some level of electrical isolation between the balls and raceways. The oil film is developed as the shaft rotation speed increases. Indeed, the bearing can be considered

in short circuit when the shaft is not rotating, in which case the balls make electrical contact with the bearing surfaces.
The bearings can be modelled as a pure capacitance, or as series or parallel capacitance-resistance. In the last two cases, the impedance behaviour is strongly capacitive. Fig. 3 shows the ball bearing schematic and its related electrical model (series capacitance-resistance). The capacitance value depends on the relative permittivity of the lubricant oil ϵ_R, vacuum permittivity ϵ_0, Hertzian area A_H and lubricant oil thickness h_0:

$$C = \epsilon_0 \epsilon_R \frac{A_H}{h_0}. \quad (1)$$

Therefore, bearings work as an impedance with a strong capacitive behaviour in "normal" operating conditions. Once the bearing voltage V_B, which depends on the V_{COM} and motor capacitances [17], exceeds the threshold dielectric limit V_{LIM}, it results in breakdown of the oil insulation and the bearing becomes conductive. This condition is referred to in this paper as the breakdown state. During this state, the bearings can be modelled as a pure resistance.
The transition between the non breakdown and breakdown states generates an impulsive current (EDM) across the bearings, which are known to strongly affect their life.

III. Experimental set-up

The proposed experimental setup is designed to measure the bearing in isolation eliminating any influence of other parasitic capacitances (winding-frame, rotor-frame, winding-rotor capacitances). The bearing under test is a SKF 61905 2RS1 with the following main dimensions: bore diameter 25 mm, outside diameter 42 mm and width 9 mm. It is a single row deep groove ball bearing which is made with stainless steel and has grease as lubricant. The bearing is inserted in a specially designed holder and coupled through its own shaft to the dynamometer shaft via a coupling. In order to electrically isolate the bearing from ground, and therefore allow the measurement of the current through the bearings only, the bearing holder is fixed to the support using a polypropylene plastic plate and nylon bolts; an electrically insulated coupling is used. The electric contact to the shaft is made using a carbon brush (motor carbon brush - BOSCH) which is held in a metallic support and insulted from the ground by plastic sheets. The experimental set-up schematic is shown in Fig. 4

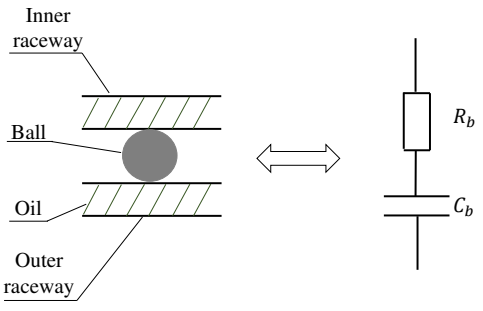

Fig. 3: Ball bearing schematic and its related electrical model.

with the test rig in Fig. 5. Several voltage amplitudes and frequencies are applied by the impedance analyzer between the shaft, using the a carbon brush which is in contact with the bearing inner raceway, and the bearing holder, which is in contact with the bearing outer raceway, for different shaft speed, generating as output the impedance (amplitude and phase), current and voltage. In order to minimize the addition of parasitic impedance to the measurements, electrical connection to the bearing holder was made using a short length of wire (50 mm), attached by screw. The short length of wire attached to the bearing holder and brush holder were in turn directly connected to the impedance analyzer with a Hioki four terminal probe (Model N.O. L2000) which has a length of 1 m. The estimated pressure acting on the brush is 28 kPa which is determined predominately by the brush holder spring rate. The shaft speed is controlled by the dynamometer. A generic procedure to test impedance, current and voltage of ball bearings under sinusoidal waveforms, while mitigating the major measurement noises, is proposed below:

- Customize shaft and holder based on bearing inner and outer diameters;
- If a coupling is needed to connect dyno and bearing shafts, it is essential to use an insulated one;
- Insulate the carbon brush and its support from the ground by dielectric sheets;
- Insulate the bearing from the ground by using a dielectric plate and bolts between the support and bearing holder;
- Use an impedance analyzer to generate the voltage and

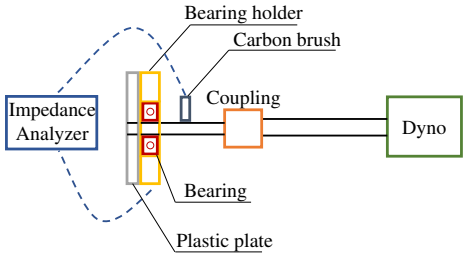

Fig. 4: Schematic of the experimental set-up.

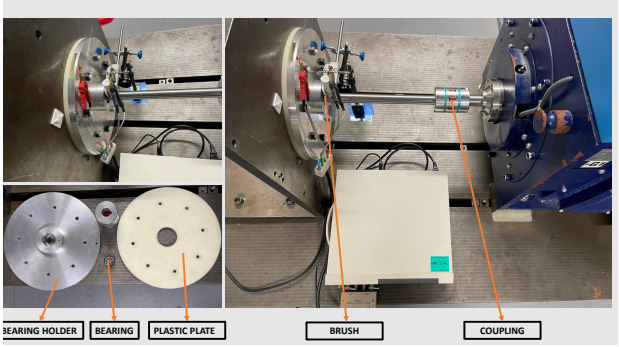

Fig. 5: Test rig: carbon brush, electrically insulted coupling, bearing holder, bearing, plastic plate and bolts, impedance analyzer.

measuring the bearing impedance.

IV. Test analysis and discussion

A statistical analysis is implemented in order to study the electrical discharge phenomenon in ball bearings. A large amount of data are generated by measuring 500 impedance values (phase and amplitude), for different applied voltage amplitude, frequency and shaft speed. The impedance analyser is able to detect these 500 values in 3 s, which means that the 'sampling' time is 6ms. Two different analyses are presented:

1) Voltage frequency sweeps from 100 kHz to 1MHz (with a step of 100 kHz) for shaft speeds of: 0, 100 and from 200 to 1600 rpm (with steps of 200 rpm), and voltage amplitude from 1 to 5 V (with steps of 1 V). Therefore, the number of data files is $500 * 10 * 10 * 5 = 250,000$ (points*frequencies*shaft speeds*voltages);
2) Voltage amplitude sweeping from 1 to 5 V (step 0.1 V) for the shaft speeds 200, 1000, 1200, 1600 rpm, and voltage frequencies 200 kHz, 1MHz. Therefore, the output data are $500 * 50 * 4 * 2 = 200,000$ (points, voltages, speeds, frequencies).

The impedance is analysed and its characterisation allows the classification into either breakdown or non-breakdown states. An additional "transition" state is introduced where no clear identification of its breakdown state is possible.

The bearing states classification in the three categories is based on the measured phase (PH) of the impedance. In particular, it is assumed that: if PH $< -70^o$ there is no breakdown. This state is indicated as "C" due to the mostly capacitive behaviour. If PH$> -20^o$ the bearing is in breakdown. This condition is indicated by "R", in reference to its mostly resistive behaviour. The range $-70^o <$PH$< -20^o$, is referred to as a transition state (T). It is worth to say that the transition state (T) does not mean necessarily that the impedance is in a transitory state between no breakdown and breakdown ones. Indeed, the bearing impedance depends strongly by oil film thickness which could be affected by other factors, such as dust. In the absence of breakdown, the bearing exhibits essentially capacitive behavior, which in the ideal case would yield a measured impedance phase of -90^o. Rather than define non-breakdown as exactly a -90^o phase shift it is necessary to introduce some degree of margin to the measured phase which is nevertheless tending to capacitive behavior. To this end, a tolerance of 20^o was applied to define a threshold of capacitive behavior, i.e for a measured impedance phase of $< -70^o$ it is assumed that the bearing is not undergoing breakdown. During breakdown, the bearing exhibits essentially resistive behaviour which corresponds, in the ideal case, to an impedance angle of 0^o. Again, it is necessary to apply some margin to the definition of breakdown to allow for non-ideal behavior of the oil-film etc. The same tolerance of 20^o was applied to the breakdown definition, i.e., a measured impedance phase between -20^o and 0^o is indicative of breakdown. This results in a transition zone of indeterminate bearing condition between -70^o to -20^o. It is recognized that this margin of 20^o at either end of the impedance phase intervals observed is somewhat arbitrary, but as will be demonstrated later in subsection IV-A, the measurements themselves tend to cluster well within these tolerance bands demonstrating the both the importance of allowing for some deviation from the ideal angles of -90^o and 0^o and the relative insensitivity of the categorization of breakdown condition to the exact margin adopted. All measurements are obtained at room temperature ($\triangleq 25^oC$) and with no mechanical load. Therefore, the temperature and load effects on the bearing impedance are not taking into the account in this article. To present the results in these three categories can help to study the impedance proprieties in a clear way, taking into the account its probabilistic behaviour. A preliminary test analysis is carried out in order to understand the carbon brush impact on the impedance frequency response. The test is proposed for an applied voltage of $1V$ and a wide frequency range from 100 kHz to 1 MHz with a step of 100 kHz when the shaft (which is made by aluminium) is not rotating. In this way, the bearing impedance can be considered in short circuit, testing the carbon brush impedance only. The preliminary analysis shows that the impedance amplitude is constant with the frequency, representing a value of 13.2Ω and a pure resistive behaviour whereas the carbon brush resistance is only 0.3Ω. It means that the contact surface between carbon brush and shaft is not perfect, creating a higher impedance. However, the total impedance can be neglected considering its small value in the context measured impedances (typically in the kΩ range at the non-breakdown condition).

A. Impedance analysis

This analysis shows the impedance phase and amplitude with respect to the frequency, and speed. Two shaft speeds are selected for the purpose: 400 and 1600 rpm. At 400 rpm, it can be seen that the impedance is capacitive for each analysed frequency at 1 V as the phase is close to $-90deg$ (Fig. 6). The impedance magnitude decreases with increasing frequency, which is indicative of the impedance being in the non-breakdown state. In contrast, at maximum impedance analyzer output voltage of 5 V (Fig. 7), the impedance is in breakdown for all frequencies, with a decreasing phase value with decreasing frequency while the amplitude is mostly constant.

The trend is confirmed also at 1600 rpm (Fig. 8 and 9) with the difference that in the non-breakdown state (Fig. 8) the impedance is "less capacitive" compared to the lower speed case at 400 rpm, especially for low frequencies.

B. Impedance value in breakdown

In this subsection, the breakdown resistance values as function of shaft speed are measured for different applied voltages. Indeed, in the breakdown state, the impedance can be considered as a mostly resistive. The analysis is carried out at 200 kHz and 1 MHz of voltage frequencies. Therefore, in order to study the resistance behaviour in breakdown, only the impedance amplitudes in the R state are taken into the account, averaging their value for each shaft speed point.

The results of the analysis are shown in Fig. 10 and 11 for 200 kHz and 1 MHz, respectively. From the proposed analysis, it can be observed that the higher the breakdown voltage,

the lower the resistance amplitude. Moreover, it is clear that for low and high shaft speeds the resistance is lower than for medium speeds. Comparing the two different frequencies under study, it is interesting to note how higher frequencies reduce the breakdown impedance (resistance) amplitude.

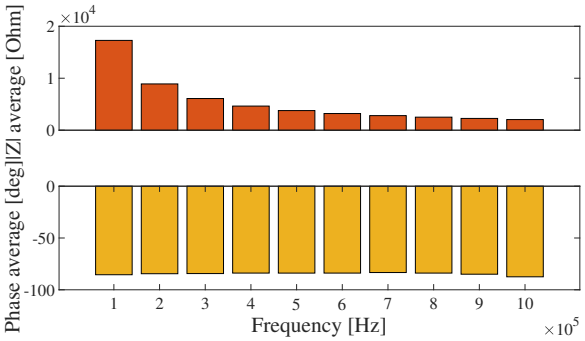

Fig. 6: Impedance against frequency at 400 rpm 1 V.

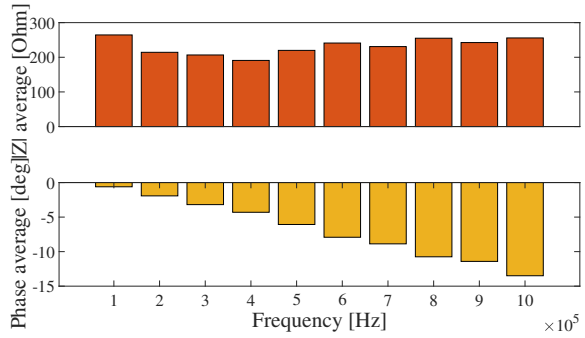

Fig. 7: Impedance against frequency at 400 rpm 5 V.

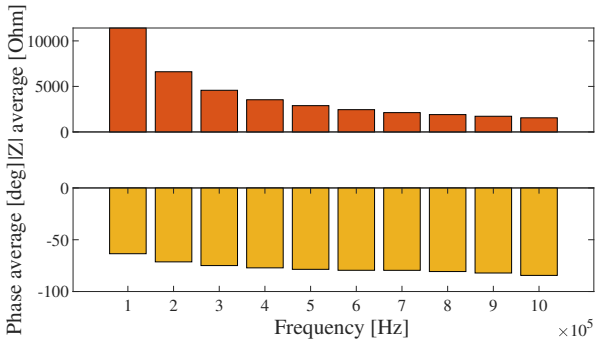

Fig. 8: Impedance against frequency at 1600 rpm 1 V.

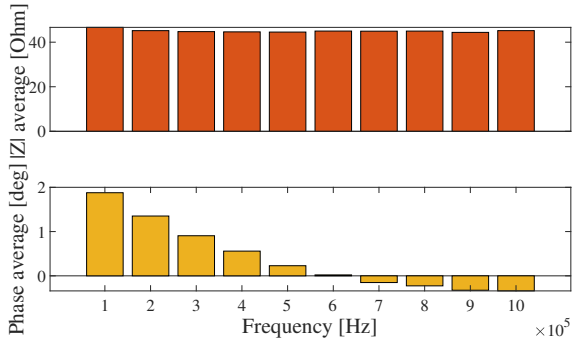

Fig. 9: Impedance against frequency at 1600 rpm 5 V.

Another interesting aspect is the relationship between shaft speed and breakdown resistance. The typical form of a Stribeck [31] curve qualitatively shown in Fig. 12 can help to understand the breakdown resistance trend against shaft speed. At very low speed ν there is a high value of friction coefficient μ because there is still contact between the balls and raceways surfaces; μ decreases with increasing of ν, reaching its minimum value for medium speeds. After this point, μ starts to increase its value with ν. Therefore, a possible interpretation of the breakdown resistance trend could be explained as following: at low speeds the breakdown is due to the contact between balls and raceways surfaces (i.e., low value of resistance); at medium speed the oil film is better distributed and the breakdown is due to only the dielectric breaking resulting in higher value of resistance; at higher speeds, the breakdown resistance value decreases due to the increased value of μ which can be translate with an higher surface contact. Another possible explanation of why the resistance values decreases with speed can be search on the dust presents into the bearing. Indeed, it could have an higher probability to impact on the surfaces compromising the oil insulation.

C. Breakdown probability

In order to understand the probability of breakdown for different frequencies, voltage amplitudes and shaft speeds, Figs. 13, 14, 15 and 16 show the analysis, using the output

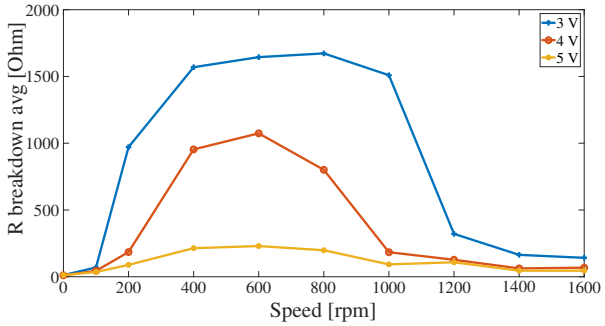

Fig. 10: Breakdown resistance amplitude for different voltage amplitudes against shaft speed at 200 kHz.

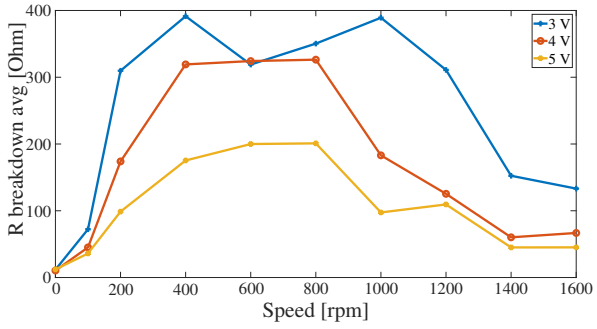

Fig. 11: Breakdown resistance amplitude for different voltage amplitudes against shaft speed at 1 MHz.

values obtained with the sweep in the voltage frequency, for the shaft speeds of 400, 800, 1200 and 1600 rpm. Therefore, 10000 values are taken into the account, 2000 for each voltage. Analysing Fig. 13 at 400rpm, it is possible to see that below 2 V there is no breakdown and the behaviour is only capacitive (C). The transition state (T) and the resistive one (R) start at 3 V with still high probabilities to have the C state whereas at 4 V the bearing impedance is almost always only in T or R states. Increasing the voltage to 5 V, it is possible to see how the bearing is always in breakdown. An interesting observation is that the breakdown probability (R state) increases with decreasing of frequency. This trend is confirmed also for the other studied shaft speeds (Figs. 14, 15, 16). Another interesting observation is that the R and T states occur for lower voltage amplitudes with increasing of shaft speeds. For example, at 3 V, the bearing is always in breakdown for the speeds 1200 and 1600 rpm whereas there is some probability of breakdown for 800 rpm and low frequency, and very low probabilities are observed for 400 rpm. Indeed, the shaft speed has a strong influence on the voltage breakdown as is shown in detail in subsection IV-E.

An explanation of why the breakdown is more likely for lower frequencies could be found in the fact that bearing impedance magnitude decreases with increasing frequency:

$$Z = R + j\frac{1}{2\pi f C}. \tag{2}$$

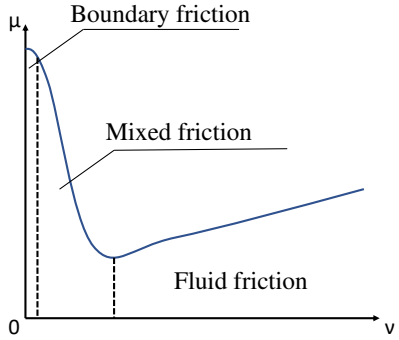

Fig. 12: Qualitative depiction of Stribeck curve [17] - μ is the friction coefficient; ν is the velocity.

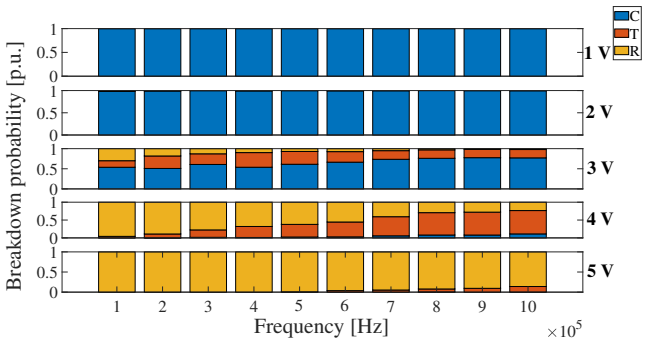

Fig. 13: Breakdown probability for different voltages against frequency at 400 rpm - C = capacitive state; T = transition state; R = resistive state.

Therefore, it is clear how the actual voltage applied on the bearing impedance is lower:

$$V_Z = V\frac{Z}{Z + R_g}. \tag{3}$$

where R_g is the signal generator internal resistance, which can be considered in series with the bearing's impedance, V is the signal voltage and V_Z is the impedance voltage.

D. Influence of frequency in breakdown

This analysis summarises the influence of voltage frequency when the bearing is in breakdown. Results are reported for 5 V,

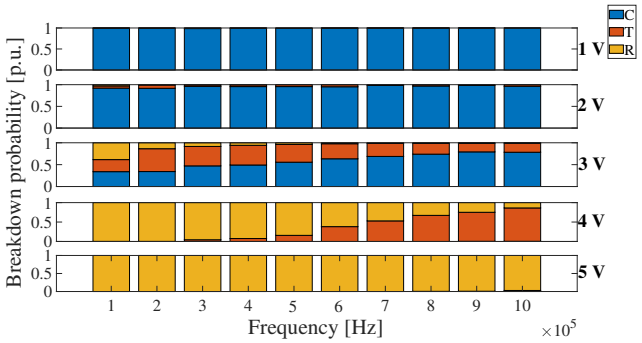

Fig. 14: Breakdown probability for different voltages against frequency at 800 rpm - C = capacitive state; T = transition state; R = resistive state.

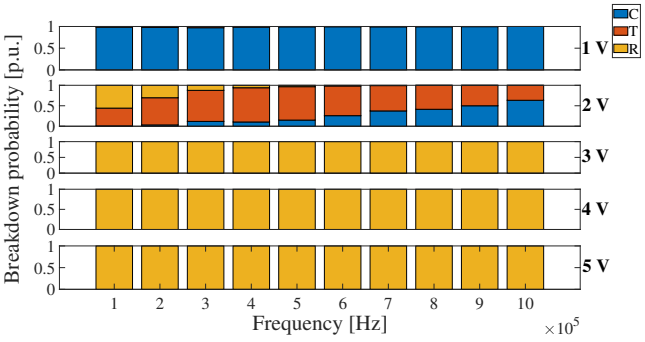

Fig. 15: Breakdown probability for different voltages against frequency at 1200 rpm - C = capacitive state; T = transition state; R = resistive state.

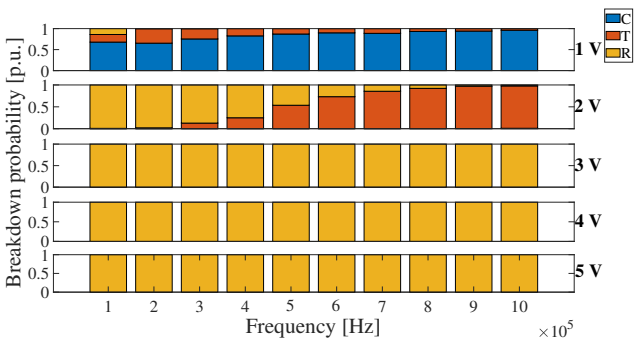

Fig. 16: Breakdown probability for different voltages against frequency at 1600 rpm - C = capacitive state; T = transition state; R = resistive state.

the voltage with the highest probability of breakdown for any frequency and shaft speeds. Fig. 17 shows the phase average against the frequency for different shaft speeds. It is clear how the lower the frequency, the closer is the phase impedance to 0^o, therefore the lower the frequency, more "resistive" is the breakdown.

E. Voltage breakdown point

This subsection investigates how the shaft speed can affect the voltage breakdown point. Measurements obtained while sweeping the voltage amplitude are presented here. Firstly, only the resistive state voltage amplitudes are considered. Secondly, only voltage values which cause the breakdown for a probability higher than 20% are used. Finally, the minimum value of this voltage is considered to be the breakdown initiation point. Fig. 18 reports the voltage breakdown for 200, 1000, 1200 and 1600 rpm at 200 kHz and 1MHz. It is clear that the shaft speed has an impact on the voltage breakdown point, exhibiting lower values for low and high speeds, and higher values for medium speeds.

V. Bearing Modelling and Validation

In order to support the calculation of bearing currents, the experimental tests are used to develop a simple bearing model which can be implemented in simulation software e.g. Simulink, as shown in Fig. 19. In order to have a validation of the model for both no breakdown (C) and breakdown (R) states, two different measured impedance values are selected at

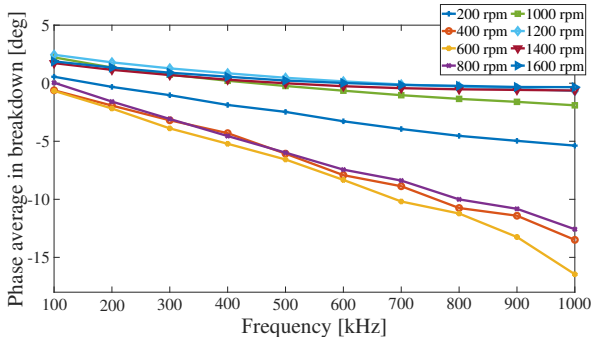

Fig. 17: Phase average in breakdown state (R) against frequency for different shaft speeds

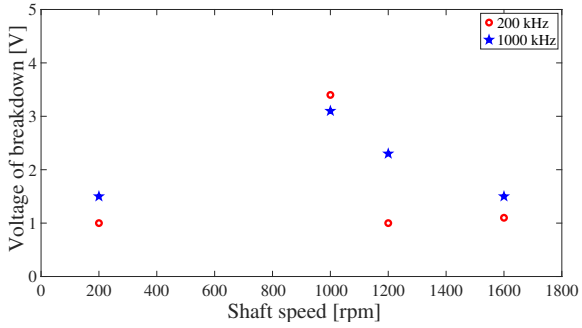

Fig. 18: Voltage breakdown point against shaft speed at 200 kHz and 1 MHz.

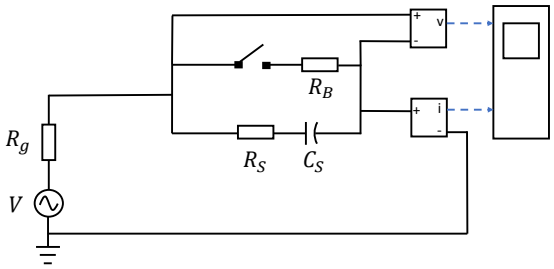

Fig. 19: Simulink bearing model: V = generator, R_g = generator inner resistance, R_S = resistance in no breakdown state, C_S = capacitance, R_B = resistance in breakdown.

the same operating conditions. Therefore, this model is only implemented to validate the proposed measurement method. As presented in section IV, the bearing breakdown occurs with a statistical probability. Therefore, the same conditions of shaft speed, voltage frequency and amplitude may or may not cause the breakdown. A simulation is presented here where there is no breakdown state from $0\mu s$ to $6\mu s$ and from $10\mu s$ to $15\mu s$. In this state, the switch is opened and the generator V is in parallel with the RC series and its inner resistance R_g. In order to simulate the breakdown state between $6\mu s$ and $10\mu s$, the switch is closed during this period. In this case, the model has the generator V in parallel to the series between its inner resistance R_g and parallel between the RC series and the breakdown resistance R_B. The simulation is carried out for the operating conditions of 1000 rpm, 3 V, 1 MHz, selecting two impedance values from the measured 500 ones: one in no breakdown and one in breakdown state. The first one presents a bearing phase impedance of -87.354^o whereas it is -12.138^o for the second one. Impedance values used for the simulation are listed in table I, where it is possible to appreciate that even in breakdown the resistance still presents a significantly large value of 255Ω due to the low breakdown voltage ($3V$).

The voltage and current waveforms for the whole period under investigation are shown in Fig. 20, where it is possible to appreciate that during the non breakdown period, the impedance is in large part capacitive with a phase shift of approximately 90^o degrees between voltage and current. On the other hand, the impedance is almost purely resistive during the breakdown state in which current and voltage are closer in phase. This trend reproduces well the experimental measurements. Observing the voltage and current amplitudes, it is possible to see that in the non breakdown case the voltage is $V_{NB} = 2.99V$ and current is $i_{NB} = 1.76mA$ whereas in breakdown they are $V_B = 2.15V$ and $i_B = 8.50mA$, respectively. Comparing these data with the experimental test ones ($V_{NB} = 2.88V$, $i_{NB} = 1.69mA$, $V_B = 2.10V$, $i_B = 8.01mA$), the voltage error is $V_{ERROR} = 3.80\%$ and current error is $i_{ERROR} = 4.14\%$ in no breakdown state whereas $V_{ERROR} = 2.38\%$ and $i_{ERROR} = 6.12\%$ in breakdown state as summarised in table II. The same simulation analysis is

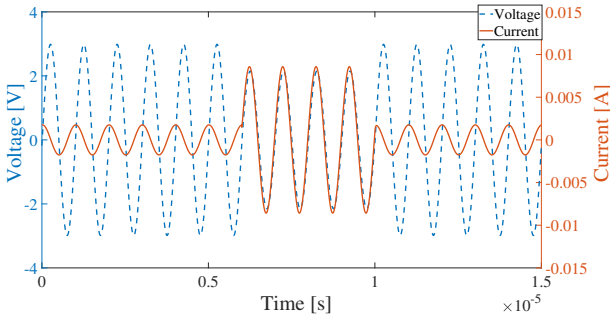

Fig. 20: Simulink simulation: voltage and current waveforms at 3V and 1000 kHz.

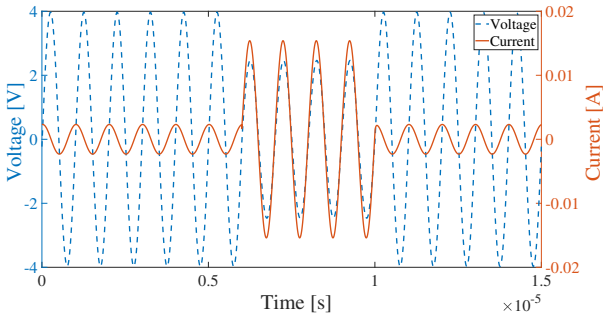

Fig. 21: Simulink simulation: voltage and current waveforms at 4V and 800 kHz.

TABLE I: Simulation values (1000 rpm-3V-1MHz)

Parameter	Value	Unit
V	3	V
f	1	MHz
C_S	$9.38\text{x}10^{-11}$	F
R_g	100	Ω
R_B	255	Ω
R_S	78.4	Ω

proposed for 800 rpm, 4 V and 1 MHz. Table III and IV summarise the input data used for the simulation and the resulting comparison, respectively whereas Fig. 21 shows the simulation output voltage and current. In this condition, the output voltage and current amplitudes are $V_{NB} = 3.96V$, $i_{NB} = 2.30mA$ in the non breakdown case whereas $V_B = 2.15V$, $I_B = 8.50V$ in the breakdown one. Comparing these results with the experimental outputs ($V_{NB} = 3.83V$, $i_{NB} = 2.22mA$, $V_B = 2.40V$, $i_B = 14.60mA$). As will be evident, there are small errors with voltage and current of $V_{ERROR} = 3.39\%$ and $i_{ERROR} = 3.60\%$ respectively in non-breakdown, with corresponding values of $V_{ERROR} = 1.25\%$ and $i_{ERROR} = 5.48\%$ in breakdown.
Finally, It is possible to affirm that the comparisons have a good match, showing the accuracy of both measurements and RC series bearing model.

VI. Additional Analysis on a Different Bearing

This section describes additional experimental analysis on a different bearing topology. The bearing under test is SKF

TABLE II: Simulation and experimental test comparison (1000 rpm-3V-1MHz)

Parameter	Simulation	Experimental test
V_{NB}	$2.99V$	$2.88V$
i_{NB}	$1.76mA$	$1.69mA$
V_B	$2.15V$	$2.10V$
i_B	$8.50mA$	$8.01mA$
$V_{NB,ERROR}$	3.80%	-
$i_{NB,ERROR}$	4.14%	-
$V_{B,ERROR}$	2.38%	-
$i_{B,ERROR}$	6.12%	-

TABLE III: Simulation values (800 rpm-4V-1MHz)

Parameter	Value	Unit
V	4	V
f	1	MHz
C_S	$9.31\text{x}10^{-11}$	F
R_g	100	Ω
R_B	162	Ω
R_S	153	Ω

TABLE IV: Simulation and experimental test comparison (800 rpm-4V-1MHz)

Parameter	Simulation	Experimental test
V_{NB}	$3.96V$	$3.83V$
i_{NB}	$2.30mA$	$2.22mA$
V_B	$2.43V$	$2.40V$
i_B	$15.40mA$	$14.60mA$
$V_{NB,ERROR}$	3.39%	-
$i_{NB,ERROR}$	3.60%	-
$V_{B,ERROR}$	1.25%	-
$i_{B,ERROR}$	5.48%	-

61905 R-2Z which has the same dimensions and many of the same features of SKF 61905 2RS1 (single row, deep grove, grease lubricant, seal cover) but with non-contact cover. The non-contact cover means that the SKF 61905 R-2Z has a lower friction than SKF 61905 2RS1. The breakdown probability for different frequencies and voltages at 400 and 800 rpm of shaft speed are shown in Figs. 22 and 23, respectively. This bearing topology presents a similar breakdown probability with respect to the higher friction variant at the same frequencies, shaft speeds and applied voltages (see Figs. 13 and 14). Therefore, the qualitative analysis on this bearing confirms results and conclusions of the analyses proposed in previous sections for the other bearing. In particular, it is confirmed that the breakdown probability increases for higher voltages and lower frequencies.

VII. Conclusion

This work has demonstrated a direct approach to measure impedance, output voltage and current of electrical machine ball bearings for different operating conditions. A large quantity of output data are obtained and processed using a statistical approach. The proposed analysis investigates the impact of shaft speed, voltage amplitude and frequency on the bearing impedance in both breakdown and non breakdown conditions. A bearing model presented to further illustrate the experimen-

tal data, comparing the output current and voltage amplitudes between the simulations and measurements.

The proposed analysis demonstrates that:

- The breakdown resistance amplitude decreases with increasing voltage amplitude and frequency;
- The breakdown probability is higher with increased voltage amplitude and decreased frequency;
- The breakdown impedance is "more resistive" (phase shift between current and voltage closer to zero degrees) with decreasing voltage frequency;
- The threshold voltage changes with the shaft speed.

Moreover, this work proposes:

- A general guideline to test bearings reducing the measurement noise;
- A RC series bearing model.

This analysis can help in understanding the impedance bearing behaviour in both breakdown and non breakdown states, and estimate the impedance breakdown probability, for different operating conditions. The methodology and modelling developed, coupled with a detailed model of the parasitic capacitive paths in the machine, can be used to predict the bearings currents in inverter driven machines. Therefore, based on the statistical method proposed in this article, future research can include novel bearing models for improved prediction of EDM currents at the machine design stage.

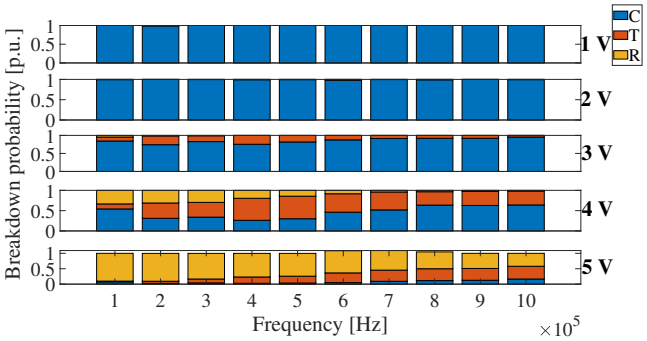

Fig. 22: Breakdown probability for different voltages against frequency at 400 rpm - C = capacitive state; T = transition state; R = resistive state.

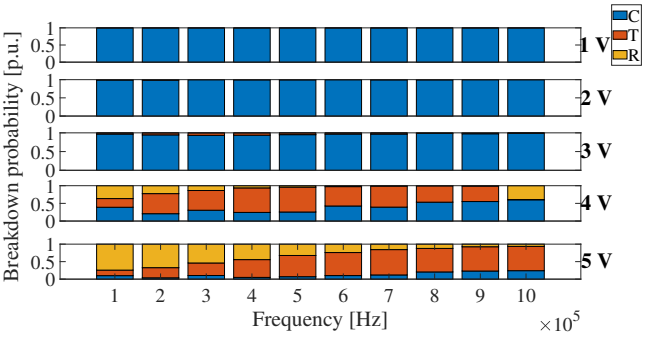

Fig. 23: Breakdown probability for different voltages against frequency at 800 rpm - C = capacitive state; T = transition state; R = resistive state.

REFERENCES

[1] Shaotang Chen, T. A. Lipo and D. Fitzgerald, "Modeling of motor bearing currents in PWM inverter drives," in IEEE Transactions on Industry Applications, vol. 32, no. 6, pp. 1365-1370, Nov.-Dec. 1996, doi: 10.1109/28.556640.

[2] S. Chen, T. A. Lipo and D. Fitzgerald, "Source of induction motor bearing currents caused by PWM inverters," in IEEE Transactions on Energy Conversion, vol. 11, no. 1, pp. 25-32, March 1996, doi: 10.1109/60.486572.

[3] I. Tsyokhla, A. Griffo and J. Wang, "Online Condition Monitoring for Diagnosis and Prognosis of Insulation Degradation of Inverter-Fed Machines," in IEEE Transactions on Ind. Electr. vol. 66, no. 10, pp. 8126 - 8135, Oct. 2019, doi: 10.1109/TIE.2018.2885740.

[4] K. R. M. N. Ratnayake and Y. Murai, "A novel PWM scheme to eliminate common-mode voltage in three-level voltage source inverter," PESC 98 Record. 29th Annual IEEE Power Electronics Specialists Conference (Cat. No.98CH36196), 1998, pp. 269-274 vol.1, doi: 10.1109/PESC.1998.701910.

[5] Y. Q. Xiang, "A novel Active Common-mode-voltage Compensator (ACCom) for bearing current reduction of PWM VSI-fed induction motors," APEC '98 Thirteenth Annual Applied Power Electronics Conference and Exposition, 1998, pp. 1003-1009 vol.2, doi: 10.1109/APEC.1998.654020.

[6] A. L. Julian, G. Oriti and T. A. Lipo, "Elimination of common-mode voltage in three-phase sinusoidal power converters," in IEEE Transactions on Power Electronics, vol. 14, no. 5, pp. 982-989, Sept. 1999, doi: 10.1109/63.788504.

[7] Shaotang Chen and T. A. Lipo, "Bearing currents and shaft voltages of an induction motor under hard- and soft-switching inverter excitation," in IEEE Transactions on Industry Applications, vol. 34, no. 5, pp. 1042-1048, Sept.-Oct. 1998, doi: 10.1109/28.720444.

[8] P. N. Tekwani, R. S. Kanchan, K. Gopakumar and A. Vezzini, "A five-level inverter topology with common-mode voltage elimination for induction motor drives," 2005 European Conference on Power Electronics and Applications, 2005, pp. 10 pp.-P.10, doi: 10.1109/EPE.2005.219191.

[9] Z. Zhao, Y. Zhong, H. Gao, L. Yuan and T. Lu, "Hybrid Selective Harmonic Elimination PWM for Common-Mode Voltage Reduction in Three-Level Neutral-Point-Clamped Inverters for Variable Speed Induction Drives," in IEEE Transactions on Power Electronics, vol. 27, no. 3, pp. 1152-1158, March 2012, doi: 10.1109/TPEL.2011.2162591.

[10] F. J. T. E. Ferreira, M. V. Cistelecan and A. T. de Almeida, "Evaluation of Slot-Embedded Partial Electrostatic Shield for High-Frequency Bearing Current Mitigation in Inverter-Fed Induction Motors," in IEEE Transactions on Energy Conversion, vol. 27, no. 2, pp. 382-390, June 2012, doi: 10.1109/TEC.2012.2187452.

[11] R. Liu, E. Yang, J. Chen and S. Niu, "Novel Bearing Current Suppression Approach in Doubly-Fed Induction Generators," in IEEE Access, vol. 7, pp. 171525-171532, 2019, doi: 10.1109/ACCESS.2019.2955803.

[12] K. Vostrov, J. Pyrhonen, M. Niemela, P. Lindh and J. Ahola, "On the application of extended grounded slot electrodes to reduce non-circulating bearing currents," in IEEE Transactions on Industrial Electronics, doi: 10.1109/TIE.2022.3172748.

[13] B. Bai, Y. Wang and X. Wang, "Suppression for Discharging Bearing Current in Variable-Frequency Motors Based on Electromagnetic Shielding Slot Wedge," in IEEE Transactions on Magnetics, vol. 51, no. 11, pp. 1-4, Nov. 2015, Art no. 8109404, doi: 10.1109/TMAG.2015.2439961.

[14] Yea, M.; Han, K.J. Modified Slot Opening for Reducing Shaft-to-Frame Voltage of AC Motors. Energies 2020, 13, 760. https://doi.org/10.3390/en13030760

[15] W. Zhu, D. De Gaetano, X. Chen, G. W. Jewell and Y. Hu, "A Review of Modeling and Mitigation Techniques for Bearing Currents in Electrical Machines With Variable-Frequency Drives," in IEEE Access, vol. 10, pp. 125279-125297, 2022, doi: 10.1109/ACCESS.2022.3225119.

[16] O. Magdun, Y. Gemeinder and A. Binder, "Investigation of influence of bearing load and bearing temperature on EDM bearing currents," 2010 IEEE Energy Conversion Congress and Exposition, 2010, pp. 2733-2738, doi: 10.1109/ECCE.2010.5618061.

[17] Y. Gemeinder, M. Schuster, B. Radnai, B. Sauer and A. Binder, "Calculation and validation of a bearing impedance model for ball bearings and the influence on EDM-currents," 2014 International Conference on Electrical Machines (ICEM), 2014, pp. 1804-1810, doi: 10.1109/ICELMACH.2014.6960428.

[18] V. Niskanen, A. Muetze and J. Ahola, "Study on Bearing Impedance Properties at Several Hundred Kilohertz for Different Electric Machine Operating Parameters," in IEEE Transactions on Industry Applications, vol. 50, no. 5, pp. 3438-3447, Sept.-Oct. 2014, doi: 10.1109/TIA.2014.2308392.

[19] O. Magdun and A. Binder, "Calculation of roller and ball bearing capacitances and prediction of EDM currents," 2009 35th Annual Conference of IEEE Industrial Electronics, 2009, pp. 1051-1056, doi: 10.1109/IECON.2009.5414669.
[20] E. Wittek, M. Kriese, H. Tischmacher, S. Gattermann, B. Ponick and G. Poll, "Capacitances and lubricant film thicknesses of motor bearings under different operating conditions," The XIX International Conference on Electrical Machines - ICEM 2010, 2010, pp. 1-6, doi: 10.1109/ICELMACH.2010.5608142.
[21] Ren, X.; Liu, R.; Yang, E. Modelling of the Bearing Breakdown Resistance in Bearing Currents Problem of AC Motors. Energies 2019, 12, 1121. https://doi.org/10.3390/en12061121
[22] J. Kalaiselvi and S. Srinivas, "Bearing current profiles in a 3-phase VSI fed induction motor drive using a simplified measurement approach," 2012 IEEE International Conference on Power Electronics, Drives and Energy Systems (PEDES), 2012, pp. 1-6, doi: 10.1109/PEDES.2012.6484374.
[23] R. Ong, J. H. Dymond and R. D. Findlay, "Comparison of techniques for measurement of shaft currents in rotating machines," in IEEE Transactions on Energy Conversion, vol. 12, no. 4, pp. 363-367, Dec. 1997, doi: 10.1109/60.638934.
[24] R. Ong, J. H. Dymond and R. D. Findlay, "Bearing damage analysis in a large oil-ring-lubricated induction machine," in IEEE Transactions on Industrial Electronics, vol. 47, no. 5, pp. 1085-1091, Oct. 2000, doi: 10.1109/41.873217.
[25] R. Ong, J. H. Dymond, R. D. Findlay and B. Szabados, "Shaft current in AC induction machine. An online monitoring system and prediction rules," in IEEE Transactions on Industry Applications, vol. 37, no. 4, pp. 1189-1196, July-Aug. 2001, doi: 10.1109/28.936413.
[26] SÄRKIMÄKI V., 'Radio Frequency Method for Detecting Bearing Currents in Induction Motors', PhD Thesis, Lappeenranta University of Technology, Finland, 2009.
[27] J. Cureño-Osornio et al., "Gradual Fault Condition Detection in the Outer Race of Induction Motor Hybrid Bearings Based on Stray Flux and LDA-FFNN Approaches," 2022 International Conference on Electrical Machines (ICEM), 2022, pp. 1809-1815, doi: 10.1109/ICEM51905.2022.9910864.
[28] Anil Kumar and C P Gandhi and Govind Vashishtha and Pradeep Kundu and Hesheng Tang and Adam Glowacz and Rajendra Kumar Shukla and Jiawei Xiang, "VMD based trigonometric entropy measure: a simple and effective tool for dynamic degradation monitoring of rolling element bearing", Measurement Science and Technology, pp. 014005, vol. 33, no. 1, Nov. 2021, IOP Publishing, doi: 10.1088/1361-6501/ac2fe8.
[29] Zhang, Yongfang and AlShorman, Omar and Irfan, Muhammad and Saad, Nordin and Zhen, D. and Haider, Noman and Glowacz, Adam and AlShorman, Ahmad, "A Review of Artificial Intelligence Methods for Condition Monitoring and Fault Diagnosis of Rolling Element Bearings for Induction Motor", Shock and Vibration, pp. 8843759, 2020, Hindawi, doi: 10.1155/2020/8843759
[30] P. Han, G. Heins, D. Patterson, M. Thiele and D. M. Ionel, "Combined Numerical and Experimental Determination of Ball Bearing Capacitances for Bearing Current Prediction," 2020 IEEE Energy Conversion Congress and Exposition (ECCE), 2020, pp. 5590-5594, doi: 10.1109/ECCE44975.2020.9235700.
[31] R. Stribeck, "Die wesentlichen Eigenschaften der Gleit- und Rollenlager (The basic characteristics of friction and roller bearings)", VDI-Journal, pp. 1341-1348, Neu Babelsberg, Germany, 1902

Daniele De Gaetano (Member, IEEE) received the bachelor's degree in Electrical Engineering from the University of Napoli "Federico II", Napoli, Italy, in 2016, the master's degree in Electrical Energy Engineering from the University of Padova, Padova, Italy, in 2018, and the Ph.D degree in Electrical and Electronic Engineering from the University of Nottingham, Nottingham, U.K., in 2022, respectively. His research as Ph.D student was focused on multiphase machines and current harmonic injection techniques for the torque capability improvement. Currently, he is a research associate within the Department of Electronic and Electrical Engineering, The University of Sheffield, Sheffield, U.K.. His main research interests include analysis, modeling and experimental tests of high frequency electrical machine bearing currents.

Wenjun Zhu received the B.Eng. degree in electrical engineering and automation from Beijing Institute of Technology, Beijing, China in 2013, the M.S. degree in sustainable energy systems from the University of Edinburgh, Edinburgh, UK in 2015, and the M.Eng. degree in electrical engineering from Beijing Institute of Technology, Beijing, China in 2016. From 2016 to 2020, he worked in the automotive industry in Shanghai, China. He is currently working toward the PhD degree in the University of Sheffield. His research interests include modelling and analysis of permanent-magnet machines and motor drive systems.

Xiangyu Sun received the B.S. and M.S. degree from Shanghai Jiao Tong University, Shanghai, China and National Tsing Hua University, Hsinchu, Taiwan in 2018 and 2021, respectively, all in electrical engineering. He is currently working towards the PH.D. degree in electrical engineering at The University of Sheffield, Sheffield, UK. His research interests include electrical machines and multi-phase motor drivers.

Xiao Chen (Member, IEEE) received the B.Eng. and M.Sc. degrees in electrical engineering from the Harbin Institute of Technology, China, in 2009 and 2011, respectively, and the Ph.D. degree in electrical machines from the University of Sheffield, U.K., in 2015. He is a Lecturer with the Electrical Machines and Drives Group, Department of Electrical and Electronics Engineering, University of Sheffield. His current research interests include manufacturing-led innovation in electrical machines, multi-phase fault tolerant electrical machines for more electric aircraft, digital twin of electrical machine and drive, high-speed electrical machines for traction, low-cost electrical machines, and powertrain energy management for electric vehicles.

Antonio Griffo (Member, IEEE) received the M.Sc. degree in electronic engineering and the Ph.D. degree in electrical engineering from the University of Napoli "Federico II", Naples, Italy, in 2003 and 2007, respectively. From 2007 to 2013, he was a Research Associate with the University of Sheffield, Sheffield, U.K., and the University of Bristol, Bristol, U.K. He is currently a professor with the Department of Electronic and Electrical Engineering, University of Sheffield. His research interests include modeling, control, and condition monitoring of electric power systems, power electronics converters, and electrical motor drives for renewable energy, automotive, and aerospace applications. He is an Associate Editor of Transactions on Industrial Electronics.

Geraint W Jewell received B.Eng. and Ph.D. degrees in electrical engineering from The University of Sheffield, Sheffield, U.K., in 1988 and 1992, respectively. Since 1994, he has been a member of Academic Staff with the Department of Electronic and Electrical Engineering, The University of Sheffield, where he is currently a Professor of Electrical Engineering, Director of the Rolls-Royce University Technology Centre in Advanced Electrical Machines and Director of the EPSRC Future Electrical Machines Manufacturing Hub. His current research interests include electrical machines, electro-mechanical actuators and electromagnetic modelling.